Atmos. Meas. Tech. Discuss., 2, 343–377, 2009
www.atmos-meas-tech-discuss.net/2/343/2009/

Atmospheric Measurement Techniques Discussions

Atmospheric Measurement Techniques Discussions is the access reviewed discussion forum of *Atmospheric Measurement Techniques*

Springtime Arctic ground-based spectroscopy of O_3 and related trace gases at Eureka, Canada – Part 1: Evaluation of the analysis method and comparison with infrared measurements

E. Farahani[1,*], K. Strong[1], R. L. Mittermeier[2], H. Fast[2], M. Van Roozendael[3], and C. Fayt[3]

[1]Department of Physics, University of Toronto, Toronto, Ontario, Canada
[2]Environment Canada, Toronto, Ontario, Canada
[3]Belgian Institute for Space Aeronomy (IASB-BIRA), Belgium
[*]now at: SPARC International Project Office, University of Toronto, Toronto, Ontario, Canada

Received: 5 November 2008 – Accepted: 19 January 2009 – Published: 16 February 2009

Correspondence to: E. Farahani (elham@atmosp.physics.utoronto.ca)

Published by Copernicus Publications on behalf of the European Geosciences Union.

Abstract

For the first time in spring 1999 the ground-based UV-visible zenith-sky measurements of stratospheric gases were performed at Environment Canada's Arctic Stratospheric Ozone Observatory (ASTRO) located at Eureka, Nunavut, Canada (80.05° N, 86.42° W, 610 m a.s.l.). The University of Toronto UV-visible ground-based spectrometer (UT-GBS) has been deployed for nine years afterwards at Eureka to measure ozone and NO_2 total columns by using sunlight scattered from the zenith sky during spring, when the conditions leading to polar ozone depletion develop. During spring 2000, elevated OClO slant column densities were also measured for the first time. First dedicated analysis of UT-GBS measurements applying two independent differential optical absorption spectroscopy algorithms was performed on spectra recorded during spring 2000. The resulting ozone and NO_2 total columns agreed to 4% and 5% or better, respectively. Also, first four years of UT-GBS results (1999–2003) were compared with those made by ozonesondes and by the Meteorological Service of Canada Fourier transform infrared spectrometer (MSC FTS) at ASTRO, which has been operated by Canada's Department of Environment for measuring the total columns of several stratospheric gases. The comparison of UT-GBS and MSC FTS ozone total columns proved to be better than 5% for the periods when both instruments were viewing similar air masses.

1 Introduction

Since 1991, UV-visible spectrometers have been part of the Network for Detection of Atmospheric Composition Change (NDACC), formerly known as the Network for Detection of Stratospheric Change (NDSC). Thus, zenith-sky observations made at a number of sites around the world provide information on stratospheric O_3 and other related species (primarily NO_2, OClO and BrO) (see van Roozendael et al., 1994; Bassford et al., 2005 and references therein). To derive column amounts, the differential optical absorption spectroscopy (DOAS) technique has been widely used (Brewer et al., 1973;

Noxon, 1975; Solomon et al., 1987; Platt, 1994). The DOAS method, which consists of ratioing a high-noon spectrum to a twilight spectrum, enhances the detectability of weak spectral features and allows the retrieval of minor stratospheric constituents such as OClO.

Ozone and NO_2 zenith-sky measurements have been made annually at Environment Canada's Arctic Stratospheric Ozone Observatory (ASTRO) every spring starting in 1999, using the University of Toronto UV-visible ground-based spectrometer (UT-GBS). ASTRO, now the Polar Environment Atmospheric Research Laboratory (PEARL), is part of the NDACC primary Arctic site located at Eureka, Nunavut, Canada (80.05° N, 86.42° W, 610 m a.s.l.) and its location is ideal for stratospheric measurements, as it lies directly below the point of maximum stratospheric variability (Harvey and Hitchman, 1996). The winter polar vortex regularly passes over ASTRO and thus measurements both inside and outside the vortex region can usually be made from this single location.

This paper is the first of two related papers that discuss stratospheric measurements in the Canadian high Arctic during 1999 to 2003 and compare the observational data set with atmospheric models. This part reports on the first dedicated analysis of the first four years of UT-GBS data set which is now a ten-year data set, providing an assessment of the retrieval algorithms and considering the relationship between O_3, NO_2 and OClO columns and potential vorticity to explain some of the observed features in the data. In addition, this is the first time that O_3 and NO_2 columns from the Meteorological Service of Canada Fourier transform infrared spectrometer (MSC FTS) measured in 1999 and 2000 are published. The MSC FTS has also been used to measure column amounts of HF, N_2O, CH_4, HNO_3, NO, and $ClONO_2$; these measurements together with more thorough explanation of differences between UT-GBS and MSC FTS results considering vortex chemistry and model-data comparisons are discussed in the second paper.

2 Instrumentation and observations

The two instruments that have been used in this work are the UT-GBS and the MSC FTS. The UT-GBS is described in detail by Bassford et al. (2005) and Farahani (2006). It consists of a triple-grating UV-visible spectrometer (Triax 180, Instruments S.A. Inc., Edison, NJ), and a CCD silicon photodetector array.

The input optics consist of a liquid light guide (LLG) (inner core=3 mm), a fused silica lens (f/2.5), and a three-lens f/# matcher as shown in Fig. 1. The spectrometer has a crossed Czerny-Turner design with aspherical optics that correct astigmatism, generate a flat field output, and provide point-to-point imaging. The spectrometer has three diffraction gratings mounted on the turret: 400, 600, and 1800 grooves/mm; Table 1 lists the gratings and their approximate spectral bandwidth and spectral resolution, while Table 2 shows the specific measurement parameters for the campaigns considered in this work. The CCD photodetector array (Instruments S.A. "Spectrum One" with a SITe chip) contains 2000×800 pixels, each 15 μm×15 μm. A thermoelectric cooling device holds the CCD at approximately −30°C. In 1999 and 2000, all 800 pixels in a column were binned on-chip, and in 2001 and 2003, the central 480 pixels were binned to reduce noise from the weakly illuminated edges of the CCD.

The UT-GBS spectra recorded in 1999 and 2000 were first preprocessed using a single bias spectrum for each campaign, which was derived from dark current measurements in the field. Daily dark current spectra were calculated as the average of the 1-s dark currents recorded after every 40 zenith-sky spectra during the day. However, during laboratory measurements in 2001, it was recognized that bias was no longer constant, therefore, during 2001 and 2003, daily bias spectra were derived from a set of dark currents recorded each night at different integration times. Corrected spectra were derived by subtracting the bias and dark current.

The MSC FTS is a Bomem DA8 spectrometer with 0.004 cm^{-1} resolution, which measures direct sun/moon light. Its spectral bandwidth is 650–5000 cm^{-1}. It has been used with a light-sensitive sun-tracking system mounted over an opening in the roof

above the spectrometer laboratory at Eureka since 1993 (Donovan et al., 1997; Farahani et al., 2007; Paton-Walsh et al., 2008). It has Mercury Cadmium Telluride (MCT) and InSb detectors with six interference filters.

The UT-GBS recorded zenith-scattered solar spectra in the wavelength range from ~320 to 620 nm during four Arctic campaigns, which took place in winter/spring at ASTRO from 1999 to 2003 with the exception of winter/spring 2002. The MSC FTS has recorded solar absorption spectra every fall and spring since 1993 at ASTRO. Here we report on MSC FTS spring measurements from 1999 to 2003.

3 UT-GBS data analysis algorithm comparison

The well-established DOAS method was used to derive O_3, NO_2, and OClO differential slant column densities (DSCDs) from the UT-GBS zenith-scattered solar spectra. The DOAS technique uses the fact that zenith-sky observations are sensitive to the stratosphere due to the stratospheric light path enhancement during twilight. In order to retrieve O_3 columns, the Chappuis band (450–540 nm) is used, while the 405–450 nm wavelength region, where the O_3 absorption is reduced, is used for NO_2 column retrieval. At the beginning of the project, the DOAS software described by Fish (1994) was adapted for UT-GBS data analysis. After the winter/spring 1999 and 2000 data sets were analysed, the more flexible WinDOAS software, which was developed at IASB/BIRA (Fayt and van Roozendael, 2001), was used for data retrieval.

Both retrieval codes use the same spectral fitting technique, DOAS, but WinDOAS has some additional features. These include a more sophisticated wavelength calibration process, which allows a more precise calibration. In our original DOAS code, first the spectrum and reference are wavelength calibrated with respect to one another using stretch and shift parameters, then both spectra are wavelength calibrated relative to the absorption cross sections of the species of interest through minimization of χ^2 of the residuals using Marquardt's method (Marquardt, 1963), which combines a parabolic expansion with a gradient search, and weights the contributions of each

according to proximity to the minimum (Fish, 1994). During the wavelength calibration process in WinDOAS, the Fraunhofer structures of the high-noon reference spectrum are aligned with those of an accurately calibrated high-resolution solar reference atlas (Kurucz et al., 1984) which is degraded to the resolution of the instrument as part of a fitting procedure. The spectral interval is divided into a number of equally spaced sub-windows in which a non-linear least squares (NLLS) fitting algorithm is applied to fit measured intensities to the solar spectrum. The atmospheric constituents' cross sections can be convolved in real-time with a user-defined variable slit function or with a variable slit function using the information obtained during the wavelength calibration process in WinDOAS. The latter is used in this work. Contrary to WinDOAS, in the original DOAS code, a constant Gaussian slit function, representative of the slit function in the middle of retrieval region, is used to convolve the atmospheric constituents' cross sections prior to the retrieval process.

In order to evaluate the WinDOAS software before applying it to the rest of the Arctic data set, the retrieval of O_3 and NO_2 DSCDs for winter/spring 2000 was performed using WinDOAS with exactly the same retrieval parameters as were used in our original DOAS software. In the top panel of Fig. 2, the measured and fitted differential optical depths (DODs) of O_3 obtained using both the original DOAS software and WinDOAS are shown (both for SZA 90° on day 88, 28 March 2000, sunrise). Figure 3 presents a comparison of NO_2 measured and fitted optical depths between DOAS and WinDOAS on the same day. As seen in these two figures, the spectral fit quality and the differential optical depths for O_3 and NO_2 improved once WinDOAS was applied to the spectra.

The RMS residuals of fitted differential optical depths of O_3 for the original DOAS analysis were calculated as 8.29×10^{-4} and 7.69×10^{-4} for sunrise and sunset (SZA=90°) on the day of the reference spectrum (day 88, 28 March 2000) respectively, which were reduced to 6.88×10^{-4} and 3.20×10^{-4} for WinDOAS analysis. On average, O_3 RMS residuals decreased by 38% for WinDOAS compared to the original DOAS code for spectra recorded in the SZA range 85° to ~94°. The RMS residuals of fitted differential optical depths of NO_2 for the original DOAS analysis were calcu-

lated as 5.23×10^{-4} and 5.32×10^{-4} for sunrise and sunset (SZA=90°) on the day of the reference spectrum (day 88, 28 March 2000) respectively, which were reduced to 3.94×10^{-4} and 4.09×10^{-4} for WinDOAS analysis. NO_2 RMS residuals decreased by 24% on average.

Another improvement in WinDOAS compared to the original DOAS software is the capability of dividing the wavelength calibration region into subregions and minimizing the residuals between the degraded solar spectrum and the reference spectrum in the subregions to achieve the best possible wavelength calibration parameters: spectral shift and first order stretch. The number of subregions that can be used in the NO_2 calibration region (405–450 nm) can be optimized by comparing the RMS residuals of the solar spectrum and calibrated reference spectrum.

WinDOAS was initially applied to all measured spectra from the Eureka 2000 field campaign. O_3 and NO_2 DSCDs were retrieved and converted to vertical column densities (VCDs) using the air mass factors (AMFs) calculated by the radiative transfer model (see Sect. 4). The mean WinDOAS O_3 VCD, shown in Fig. 4, is 4% less than the mean O_3 VCD from the original DOAS retrieval code, which is within the nominal ±5% measurement errors (discussed further in Sect. 4). Another point to mention is that WinDOAS retrieval of O_3 columns was possible for day 55 (24 February 2000), two days after polar sunrise at Eureka, however the poor quality of the twilight spectra combined with the less accurate wavelength calibration process in the original DOAS code prevented the retrieval of O_3 VCDs for the same day with this code.

Applying the WinDOAS algorithm to spectra in the NO_2 region resulted in the retrieval of 11 more twilight periods during the 2000 field campaign compared to the existing DOAS results because of the more accurate wavelength calibration process and the wavelength-dependent slit function parameter in WinDOAS. Figure 5 shows the complete time series of the retrieved NO_2 VCDs from UT-GBS measurements during winter/spring 2000 at ASTRO. DOAS-WinDOAS comparisons for NO_2 columns were more challenging for the first part of the campaign, soon after polar sunrise at Eureka (days 55 to 62). During this period the NO_2 levels are low; thus the less precise wave-

length calibration process in the existing DOAS code resulted in poor quality spectral fits, which did not capture the NO_2 DSCDs accurately. In Fig. 5, the mean WinDOAS NO_2 VCD is 5% less than the mean NO_2 VCD resulting from the original DOAS code, which is better than the nominal measurement error of ±12% in which the systematic component of the error is also considered (discussed further in Sect. 4).

4 Final data retrieval

4.1 UT-GBS

The corrected twilight spectra for SZAs from 80° to ~94° during both sunrise and sunset were considered for the retrieval of O_3, NO_2 and OClO DSCDs. Using WinDOAS software, UT-GBS zenith-scattered spectra were calibrated in the wavelength range 405 to 545 nm for 1999, 2001 and 2003 against a common reference spectrum for each year. However the wavelength range for calibration was extended from 360 to 545 nm in 2000 to provide the opportunity for retrieving the elevated levels of OClO during this cold spring. The reference spectra were recorded at high noon under clear sky conditions. The absorption cross sections of O_3 at 241 K (Burrows et al., 1999), NO_2 at 241 K (Burrows et al., 1998), OClO at 204 K (Wahner et al., 1987), O_4 at 298 K (Greenblatt et al., 1990), BrO at 228 K (Wahner et al., 1988) and H_2O at 296 K (Rothman et al., 1998) were smoothed using a wavelength-dependent Gaussian slit function parameter, which was determined in the wavelength calibration process by a cubic polynomial fit.

The Ring effect is a phenomenon causing the infilling of the solar Fraunhofer lines in the scattered daylight spectrum (Grainger and Ring, 1962). In order to deal with the Ring effect, which has been shown to be mostly due to rotational Raman scattering (Chance and Spurr, 1997; Vountas et al., 1998; Sioris et al., 2002), it is considered as a pseudo-absorber and a Ring cross section is calculated using the model of Chance and Spurr (1997).

Converting the retrieved O_3 and NO_2 DSCDs to VCDs requires accurate knowledge

of the transfer of radiation through the atmosphere for the calculation of the appropriate AMFs. The radiative transfer (RT) model used for O_3 and NO_2 AMF calculations is described in detail by McLinden (1998) and McLinden et al. (2002). This model solves the radiative transfer equation using successive orders of scattering in an inhomogeneous atmosphere. The radiance of photons which are scattered once, twice, three times and so on is calculated iteratively, with the total radiance taken as the sum over all scattering orders. The RT model geophysical inputs are vertical profiles of air number density, temperature, absorber number density, aerosol number density, aerosol size distributions, refractive indices and surface albedo (McLinden, 1998; Bassford et al., 2001). In this work averaged profiles from 11 ozonesondes were used for temperature and absorber number density. The input parameter for the type of surface was set to Lambertian with 0.7 albedo appropriate for the high Arctic and the no cloud option was chosen. Langley plots of DSCDs versus AMF were used to derive the O_3 VCDs, as O_3 is a diurnally slowly-varying species (Sarkissian et al., 1997).

Deriving NO_2 VCDs from NO_2 SCDs is more challenging because NO_2 changes through twilight so it requires accurate knowledge of the AMFs. Also the amount of NO_2 in the reference spectrum, the reference column density (RCD), needs to be derived. The RCD value can be either calculated using a chemical box model or can be determined independently of a model by using observed DSCD values. In this work, NO_2 RCDs were determined by using pseudo-Langley plots of NO_2 differential slant column densities versus NO_2 AMFs in the SZA range of 80°–85°, where the change in NO_2 column due to photodissociation is expected to be small (Vaughan et al., 2006). Thus, this relationship is approximately linear and the intercept represents the negative NO_2 RCD. The NO_2 RCD for each campaign is the average of RCDs for all days during that campaign. Then the NO_2 VCD at twilight, for SZA 90° is calculated using the following Equation:

$$\mathrm{VCD}(\theta) = \frac{\mathrm{DSCD}(\theta) + \mathrm{RCD}}{\mathrm{AMF}(\theta)} \quad (1)$$

where θ is the SZA. The total error for UT-GBS O_3 and NO_2 measurements was estimated from the root-sum-square of individual errors. These errors are summarized in Table 3 (Bassford et al., 2005; Farahani, 2006).

4.2 MSC FTS

The retrieval of column amounts from MSC FTS atmospheric absorption spectra is based on the SFIT1 spectral fitting routine (Rinsland et al., 1982, 1988). SFIT1.09e was applied to narrow spectral microwindows containing absorption features of the target molecules. Each FTS spectrum is a coaddition of four interferograms over 700 s, from which total columns of HF, CH_4, N_2O, O_3, HCl, NO, NO_2, $ClONO_2$, HNO_3, CFC-11, ClO, and COF_2 can be retrieved using the SFIT1 spectral fitting routine (Rinsland et al., 1982, 1988). To calculate the synthetic spectra with SFIT1, we adopted the line parameters in the HITRAN 1992 compilation (Rothman et al., 1992). The set of a priori volume mixing ratio (VMR) profiles (REFTOON41) is based on mid-latitude balloon measurements (Peterson and Margitan, 1995) but modified for the high-latitude location of Eureka. Temperature, pressure and relative humidity profiles were obtained from radiosondes launched twice daily from Eureka. Above the maximum sonde altitude, the profiles of temperature and pressure are extended to approximately 50 km with data from the US National Center for Environmental Predictions (NCEP). Above 50 km the winter sub-Arctic US Standard Atmosphere is used to 100 km.

A mean daily vertical column was calculated from the individual MSC FTS column measurements for different species at ASTRO from two or more spectra recorded each day. Error estimates for the retrieved columns were determined according to the method described by Murphy et al. (2001), to account for instrument effects, choice of algorithm, microwindows, line parameters, apriori volume mixing ratio profiles, and uncertainty in the temperature profile. Added in quadrature, this resulted in a total uncertainty of ±9.8% for O_3 and ±22.9% for NO_2.

AMTD
2, 343–377, 2009

5 Results and discussion

Ninety five days of O_3 differential slant column densities and vertical column densities were derived from UT-GBS measurements using Langley plots from March 1999 to April 2003. NO_2 differential slant column densities and vertical column densities were retrieved during 1999 and 2000, resulting in a total of 112 twilight measurements: 50 sunrise and 62 sunset. Northern Hemisphere maps of potential vorticity (PV) on 475 and 550 K isentropic surfaces were used to provide information on the dynamical conditions over ASTRO and/or interesting observational periods where O_3 columns deviated from the climatological mean. For the period from 1999 to 2003, maps of PV from the ECMWF daily analyses are used. ECMWF uses a 3-D variational analysis at T106 resolution and 60 levels in the vertical. A description of the data is given in Fahre-Vik (2003). Also for the first time at Eureka, OClO slant columns were derived from UT-GBS zenith–scattered spectra from day 55 to 89 during the cold winter of 2000.

5.1 Ozone total columns

Figure 6 shows UT-GBS O_3 vertical columns compared with Eureka ozonesonde data (for which a correction was added above the maximum sonde altitude) and MSC FTS measurements. During spring 1999, UT-GBS O_3 vertical columns compare well with MSC FTS measurements and integrated O_3 sonde profiles, agreeing within the combined measurement errors for all but two days. Figure 7 shows that the polar vortex is weak in 1999, thus the higher O_3 columns observed prior to day 91 may originate from the O_3-rich air mass of mid-latitudes.

During winter/spring 2000, UT-GBS O_3 vertical columns again agree with integrated O_3 sonde profiles and MSC FTS measurements within errors. The Eureka 2000 field season was the only cold winter among the four winters observed in this work, although there were several exceptionally cold and strong springtime vortices in the mid-1990s (Manney et al., 2005). ECMWF potential PSC areas at 475 K shown in Fig. 8 indicate potential for PSC formation above Eureka during 11–22 February 2000 (days 42–53).

AMTD
2, 343–377, 2009

At the start of the campaign, if we look at integrated sonde and UT-GBS values for days 54–57, O_3 columns are ∼350 DU, which is 13% lower than the climatological mean resulting from the Canadian Middle Atmosphere Model (CMAM) climatological chemical fields (see second paper in this set, Farahani et al. (2009) as CMAM mean within 1σ. HNO_3 measurements at Eureka unfortunately did not start until day 57 due to the solar illumination requirements and after that day there is no evidence of denitrification in the HNO_3 measurements. However, the measured HNO_3 columns remained lower than the CMAM climatological mean for much of the season in 2000, which may imply the presence of high amounts of active chlorine (see the second paper in this set, Farahani et al., 2009).

After day 72, based on ECMWF PV maps shown in Fig. 9, the polar vortex is located over Eureka as seen on the 475 K isentropic surface and stays in place until day 77 (17 March 2000). Again, based on Fig. 9, the vortex moves over Eureka on day 79 (19 March 2000) and remains over Eureka until day 89 (29 March 2000). During both periods, the observed O_3 columns fall below 300 DU as seen in Fig. 6.

During winter/spring 2001, MSC FTS O_3 vertical columns are in agreement with UT-GBS measurements except the first three coincident days when the UT-GBS shows a 30% reduction in total O_3 column which most probably is due to a localized event.

During February and March 2003, before the O_3-depleted air typical of the isolated cold vortex air mass moves over Eureka as shown in Fig. 10, UT-GBS O_3 columns are in agreement with MSC FTS columns within measurement errors. However, afterwards Eureka was located at the edge of the vortex on day 91 (1 April 2003) and inside the vortex until day 107 (18 April 2003), as is shown in Fig. 10. For this period, MSC FTS reports O_3 columns which are ∼20% higher than UT-GBS measurements; however it should be noted that the FTS has a different viewing times and geometry. Also previous O_3 column comparison between infrared and UV-visible measurements has shown differences as large as 30%, which may be partly attributed to spectroscopy (Taylor et al., 2007).

5.2 NO_2 total columns

Figure 11 shows UT-GBS NO_2 columns for 1999 and 2000 for sunrise and sunset (SZA 90°) along with NO_2 columns from the MSC FTS. The MSC FTS measured daily NO_2 columns by averaging over two or more measured values during the day. Comparison with the MSC FTS was possible during February and at the beginning of March as MSC FTS measurements were done in the SZA range of 85° to 89°, which was close in time to the UT-GBS twilight measurements. However by the beginning of April, the MSC FTS measured at higher SZAs. As expected, the daytime NO_2 columns measured by the MSC FTS are smaller than the twilight values, consistent with the NO_2 diurnal cycle and differing spectroscopic parameterization between the infrared and UV-visible measurements (Taylor et al., 2007).

5.3 OClO slant columns

A novel measurement at ASTRO was that of chlorine dioxide (OClO) DSCDs during winter/spring 2000 using UT-GBS zenith-scattered twilight spectra. The zenith-sky spectra were recorded using the 1800 grooves/mm grating by alternating between this grating and the 600 grooves/mm grating from day 55 to 89 during the cold winter of 2000. These spectra were used for retrieval of OClO DSCDs in the wavelength region 365 to 390 nm where OClO absorption features are located. Figure 12 shows the OClO measured and fitted differential optical depth and its residual for sunrise SZA 90° on day 88 (28 March 2000). OClO DSCDs were derived at SZA 90° sunrise and sunset for the period of observation and are presented in Fig. 13. The OClO slant column values are consistent with values reported in the Arctic ($\sim 2.5 \times 10^{14}$ molec/cm^2) by other studies (Kuhl et al., 2004).

6 Conclusions

Ground-based UV-visible zenith-sky spectroscopic measurements of O_3, NO_2 and OClO columns were made for the first time at Eureka using a triple-grating spectrometer deployed at ASTRO, during winter/spring of 1999–2003. An assessment of the original DOAS algorithm versus the more flexible WinDOAS was performed using the UT-GBS spectra recorded during winter/spring 2000, which resulted in an agreement of better than 4% for mean O_3 VCDs and 5% for mean NO_2 VCDs. The use of the WinDOAS algorithm for DSCD retrieval allowed the fitting procedure to be optimized and increased the possibility of retrieving DSCDs during the period right after polar sunrise. Thus, 95 days of O_3 DSCDs and VCDs were derived from UT-GBS measurements using Langley plots from March 1999 to April 2003. NO_2 DSCDs and VCDs were retrieved during 1999 and 2000, resulting in a total of 112 twilight measurements: 50 sunrise and 62 sunset.

The UV-visible O_3 and NO_2 measurements were compared with the co-located infrared measurements made during the same period using the MSC FTS. The comparison of ozone total columns proved to be better than 5% for the periods when both instruments were viewing similar air masses. The UT-GBS total O_3 columns generally agreed with sonde measurements. Low O_3 columns during the cold winter/spring of 2000 were explained using ECMWF PV and temperature data.

For the first time, OClO DSCDs were retrieved from UV-visible measurements in the Canadian high Arctic during winter/spring 2000. The OClO slant column values are consistent with values reported in the Arctic ($\sim 2.5 \times 10^{14}$ molec/cm^2). A companion paper (Farahani et al., 2009) provides a more detailed discussion of the Eureka measurements, focussing on comparison with the Canadian Middle Atmosphere Model.

Acknowledgements. The Eureka ASTRO facility was operated by Meteorological Service of Canada and the authors would like to express their gratitude to people who worked there. The authors are also indebted to Mathew Bassford for the 1999 and 2000 campaigns, and Annemarie Fraser, Stella Melo, Jeffery Taylor and Mathew Toohey for helping with the 2001 and 2003 campaigns at Eureka. The research described here was financially supported by the Canadian Foundation for Climate and Atmospheric Sciences, the Northern Scientific Training Program, the Canadian Northern Studies Trust, the Natural Sciences and Engineering Research Council of Canada, and the Meteorological Service of Canada.

References

Bassford, M. R., McLinden, C. A., and Strong, K.: Zenith-sky observations of stratospheric gases: The sensitivity of air mass factors to geophysical parameters and the influence of tropospheric clouds, J. Quant. Spectros. Radiat. Transfer, 68, 657–677, 2001. 351, 364

Bassford, M. R., Strong, K., McLinden, C. A., and McElroy, C. T.: Ground-based measurements of ozone and NO_2 during MANTRA 1998 using a new zenith-sky spectrometer, Atmos.-Ocean, 43, 325–338, 2005. 344, 346, 352

Brewer, A. W., McElroy, C. T., and Kerr, J. B.: Nitrogen dioxide concentrations in the atmosphere, Nature, 246, 129–133, 1973. 344

Burrows, J. P., Dehn, A., Deters, B., Himmelmann, S., Richter, A., Voigt, S., and Orphal, J.: Atmospheric remote-sensing reference data from GOME: Part 1- Temperature dependent absorption cross-sections of NO_2 in the 231–794 nm range, J. Quant. Spectrosc. Radiat. Transfer, 60, 1025–1031, 1998. 350, 364

Burrows, J. P., Richter, A., Dehn, A., Deters, B., Himmelmann, S., Voigt, S., and Orphal, J.: Atmospheric remote-sensing reference data from GOME: Part 2- Temperature dependent absorption cross-sections of O_3 in the 231–794 nm range, J. Quant. Spectrosc. Radiat. Transfer, 61, 509–517, 1999. 350, 364

Chance, K. V. and Spurr, R. J. D.: Ring effect studies: Rayleigh scattering, including molecular parameters for rotational Raman scattering, and the Fraunhofer spectrum, Appl. Optics, 36, 5224–5230, 1997. 350

Donovan, D. P., Fast, H., Makino, Y., Bird, J. C., Carswell, A. I., Davies, J., Duck, T. J., Kaminski, J. W., McElroy, C. T., Mittermeier, R. L., Pal, S. R., Savastiouk, V., Velkov, D., and Whiteway,

J. A.: Ozone, column ClO, and PSC measurements made at the NDSC Eureka observatory (80°N, 86°W) during the spring of 1997, Geophys. Res. Lett., 24, 2709–2712, 1997. 347
FahreVik, A.: NADIR News, Vol. 2, Norwegian Institute for Air Research, 2003. 353
Farahani, E.: Stratospheric composition measurements in the Arctic and at mid-latitudes and comparison with chemical fields from atmospheric models, University of Toronto, Toronto, Canada, Ph.D. Thesis, 2006. 346, 352
Farahani, E., Fast, H., Mittermeier, R. L., Makino, Y., Strong, K., McLandress, C., Shepherd, T. G., Chipperfield, M. P., Hannigan, J. W., Coffey, M. T., Mikuteit, S., Hase, F., Blumenstock, T., and Raffalski, U.: Nitric acid measurements at Eureka, Thule and Kiruna obtained in winter 2001/2002 using solar and lunar Fourier transform infrared absorption spectroscopy and comparison with results from three-dimensional models, J. Geophys. Res., 112, D01305, doi:10.1029/2006JD007096, 2007. 347
Farahani, E., Strong, K., Mittermeier, R. L., Fast, H., McLandress, C., Shepherd, T. G., and Chipperfield, M. P.: Springtime Arctic measurements of trace gases from 1999 to 2003 at Eureka, Canada – Part 2: Comparisons with results from three-dimensional models, in preparation, 2009.
Fayt, C. and van Roozendael, M.: WinDOAS 2.1 –Software user manual, BIRA-IASB, Uccle, Belgium, 2001. 347
Fish, D. J.: Measurements of stratospheric composition using ultraviolet and visible spectroscopy, Cambridge University Press, Cambridge, UK, Ph.D. Thesis, 1994. 347, 348
Fish, D. J. and Jones, R. L.: Rotational Raman scattering and the Ring effect in zenith-sky spectra, Geophys. Res. Lett., 22, 811–814, 1995. 364
Grainger, J. F. and Ring, J. F.: Anomalous Fraunhofer line profiles, Nature, 193, p. 762, 1962. 350
Greenblatt, G. D., Orlando, J. J., Burkholder, J. B., and Ravishankara, A. R.: Absorption measurements of oxygen between 330 and 1140 nm, J. Geophys. Res., 95, 18577–18582, 1990. 350
Harvey, V. L. and Hitchman, M. H.: A climatology of the Aleutian High, J. Atmos. Sci., 53, 2088–2101, 1996. 345
Kuhl, S., Dornbrack, A., Wilms-Grabe, W., Sinnhuber, B. M., Platt, U., and Wagner, T.: Observational evidence of rapid chlorine activation by mountain waves above Northern Scandinavia, J. Geophys. Res., 109, D22309, doi:10.1029/2004JD004797, 2004. 355
Kurucz, R. L., Furenlid, I., Brault, J., and Testerman, L.: Solar flux atlas from 296 nm to 1300

nm, National Solar Observatory Atlas No. 1, 1984. 348
Manney, G. L., Kruer, K., Sabutis, J. L., Sena, S. A., and Pawson, S.: The remarkable 2003/2004 winter and other recent warm winters in the Arctic stratosphere since the late 1990s, J. Geophys. Res., 110, D04107, doi:10.1029/2004JD005367, 2005. 353
Marquardt, D. W.: An algorithm for least-squares estimation of nonlinear parameters, J. Soc. Ind. Appl. Math., 11, 431–441, 1963. 347
McLinden, C. A.: Observation of atmospheric composition from NASA ER-2 spectroradiometer measurements, York University, Toronto, Canada, Ph.D. Thesis, 1998. 351
McLinden, C. A., McConnell, J. C., Griffioen, E., and McElroy, C. T.: A vector radiative transfer model for the Odin/OSIRIS project, Can. J. Phys., 80, 375–393, 2002. 351
Murphy, C., Bell, W., Woods, P., Demoulin, P., Galle, B., Mellqvist, J., Arlander, W., Notholt, J., Goldman, A., Toon, G. C., Blavier, J. F., Sen, B., Coffey, M. T., Hannigan, J. W., Mankin, W. G., Jones, N., Griffith, D., Meier, A., Blumenstock, T., Fast, H., Mittermeier, R., and Makino, Y.: Validation of NDSC measurements of ozone, reservoir compounds and dynamical tracers: Results of a series of side-by-side instrument intercomparisons, NDSC 2001 Symposium, Arcachon, France, 24–27 September, 2001. 352
Noxon, J. P.: Nitrogen dioxide in the stratosphere and troposphere measured by groundbased absorption spectroscopy, Science, 189, 547–549, 1975. 345
Paton-Walsh, C., Mittermeier, R. L., Bell, W., Fast, H., Jones, N. B., and Meier, A.: An intercomparison of ground-based solar FTIR measurements of atmospheric gases at Eureka, Canada, JAOTech, 2028–2036, doi:10.1175/2008JTECHA1060.1, 2008. 347
Peterson, D. B. and Margitan, J. J.: Upper atmospheric research satellite correlative measurement program (UARS-CMP) balloon data Atlas, NASA, Washington, D.C., 1995. 352
Pfeilsticker, K., Arlander, D. W., Burrows, J. P., Erle, F., Gil, M., Goutail, F., Hermans, C., Lambert, J. C., Platt, U., Pommereau, J. P., Richter, A., Sarkissian, A., van Roozendael, M., Wagner, T., and Winterrath, T.: Intercomparison of the influence of tropospheric clouds on UV-visible absorptions detected during the NDSC intercomparison campaign at OHP in June 1996, Geophys. Res. Lett., 26, 1169–1172, 1999. 364
Platt, U.: Air Monitoring by Spectroscopic Techniques, edited by: Sigrist, M. W., John Wiley and Sons Inc., London, UK, 1994. 345
Rinsland, C. P., Smith, M. A. H., Rinsland, P. L., Goldman, A., Brault, J. W., and Stokes, G. M.: Ground-based infrared spectroscopic measurements of atmospheric hydrogen cyanide, J. Geophys. Res., 87, 11119–11125, 1982. 352

Rinsland, C. P., Goldman, A., Murcray, F. J., Murcray, F. H., Blatherwick, R. D., and Murcray, D. G.: Infrared measurements of atmospheric gases above Mauna Loa, Hawaii, in February 1987, J. Geophys. Res., 91, 12607–12626, 1988. 352

Rothman, L. S., Gamache, R., Tipping, R., Rinsland, C., Smith, M., Benner, D., Devi, V., Flaud, J., Camypeyret, C., Perrin, A., Goldman, A., Massie, S., Brown, L., and Toth, R.: The HITRAN molecular database – Editions of 1991 and 1992, J. Quant. Spectros. Radiat. Transfer, 48, 469–507, 1992. 352

Rothman, L. S., Rinsland, C. P., Goldman, A., Massie, S. T., Edwards, D. P., Flaud, J. M., Perrin, A., Camy-Peyret, C., Dana, V., Mandin, J. Y., Schroeder, J., McCann, A., Gamache, R. R., Wattson, R. B., Yoshino, K., Chance, K., Jucks, K., Brown, L. R., Nemtchinov, V., and Varanasi, P.: The HITRAN molecular spectroscopic database and HAWKS (HITRAN Atmospheric Workstation): 1996 Edition, J. Quant. Spectros. Radiat. Transfer, 60, 665–710, 1998. 350

Sarkissian, A., Vaughan, G., Roscoe, H. K., Bartlett, L. M., O'Connor, F. M., Drew, D. G., Hughes, P. A., and Moore, D. M.: Accuracy of measurements of total ozone by a SAOZ ground-based zenith sky visible spectrometer, J. Geophys. Res., 102, 1379–1390, 1997. 351

Sioris, C. E., Evans, W. F. J., Gattinger, R. L., McDade, I. C., Degenstein, D. A., and Llewellyn, E. J.: Ground-based Ring-effect measurements with the OSIRIS development model, Can. J. Phys., 80, 483–491, 2002. 350

Solomon, S., Schmeltekopf, A. L., and Sanders, R. W.: On the interpretation of zenith sky absorption measurements, J. Geophys. Res., 92, 8311–8319, 1987. 345

Taylor, J. R., Strong, K., McLinden, C. A., Degenstein, D. A., and Haley, C. S.: Comparison of OSIRIS stratospheric NO_2 and O_3 measurements with ground–based Fourier transform spectrometer measurements at the Toronto atmospheric observatory, Can. J. Phys., 85, 1301–1316, 2007. 354, 355

van Roozendael, M., de Maziere, M., and Simon, P. C.: Ground-based visible measurements at the Jungfrujoch station since 1990, J. Quant. Spectrosc. Radiat. Transfer, 52, 231–240, 1994. 344

Vaughan, G., Quinn, P. T., Green, A. C., Bean, J., Roscoe, H. K., van Roozendael, M., and Goutail, F.: SAOZ measurements of stratospheric NO_2 at Aberystwyth, 1991–2004, J. Env. Monitoring, 8(3), 353–361, 2006. 351

Vountas, M., Rozanov, V., and Burrows, J.: Ring effect: Impact of rotational Raman scattering

on radiative transfer in earth's atmosphere, J. Quant. Spectros. Radiat. Transfer, 60, 943–961, 1998. 350

Wahner, A., Tyndall, G. S., and Ravishankara, A. R.: Absorption cross section for OClO as a function of temperature in the wavelength range 240–480 nm, J. Phys. Chem., 91, 2734–2738, 1987. 350

Wahner, A., Ravishankara, A. R., Sander, S. P., and Friedl, R. R.: Absorption cross section for BrO between 312 and 385 nm at 298 and 223 K, Chem. Phys. Lett., 152, 507–511, 1988. 350

Table 1. Measured values of the bandwidth of the UT-GBS for the 100 μm slit width and the FWHM spectral resolution in the middle of the CCD used for the Arctic observations.

Grating (grooves/mm)	Spectral Bandwidth (nm)	FWHM (nm)
400	300	0.96–1.28 (1999-2003)
600	234	0.78–0.96 (2000–2003)
1800	66	0.20–0.49 (1999–2003)

Table 2. Measurement parameters for the four UT-GBS campaigns.

Campaign Year	Grating (grooves/mm)	Spectral Range (nm)	CCD Mean T (K)	Reference Spectrum (SZA)
1999	400	270–625	235	24 March (79°)
2000	1800 swapping with 600	315–380 310–550	245	29 March (76°)
2001	600	330–560	232	16 April (72°)
2003	600	340–580	242	9 April (73°)

Table 3. Sources of error and error estimates for the UT-GBS O_3 and NO_2 VCDs.

Error	O_3	NO_2	Source
Random noise	1%	2%	Statistically calculated from measurements
Instrument error	3%	3%	Informed estimate
Pseudo-random errors	1–2%	4–6%	Derived from measurements
Absolute cross sections	2.6%	2.3%	Burrows et al. (1999, 1998), respectively
Temperature dependence of the NO_2 cross section	–	≤8%	Pfeilsticker et al. (1999)
Uncertainty in NO_2 RCD	–	3–7%	Derived from measurements
AMF error	3%	5–7%	Calculated for the RT model, Bassford et al. (2001)
Uncertainty in the slope of Langley plots	0.5%	–	Derived from measurements
Filling in of absorption by Raman scattering	1%	5%	Fish and Jones (1995); Pfeilsticker et al. (1999)
Total RMS error	±5–6%	±12–15%	

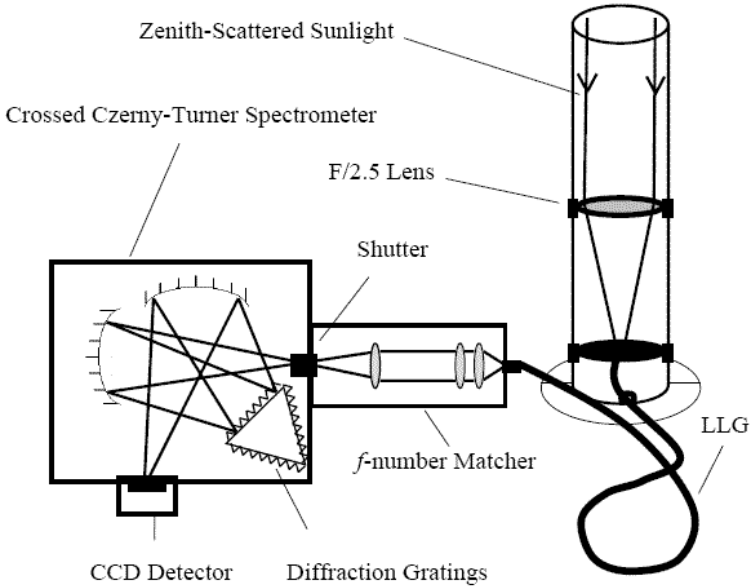

Fig. 1. Basic elements and ray diagram of the University of Toronto ground-based UV-visible zenith-sky spectrometer.

AMTD
2, 343–377, 2009

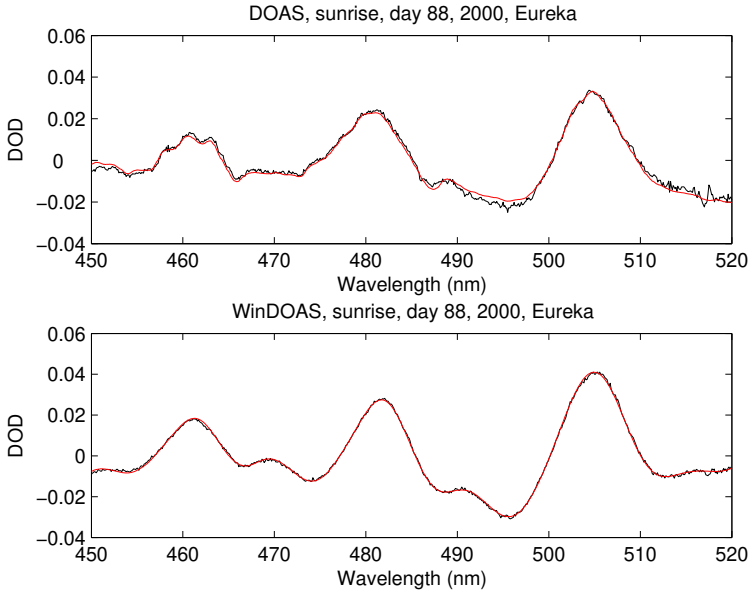

Fig. 2. Differential optical depths for O_3 (measured in black and fitted in red) at SZA 90° for UT-GBS zenith-sky measurements made on day 88 (28 March 2000), sunrise at Eureka: (top) using the existing DOAS software and (bottom) using WinDOAS software.

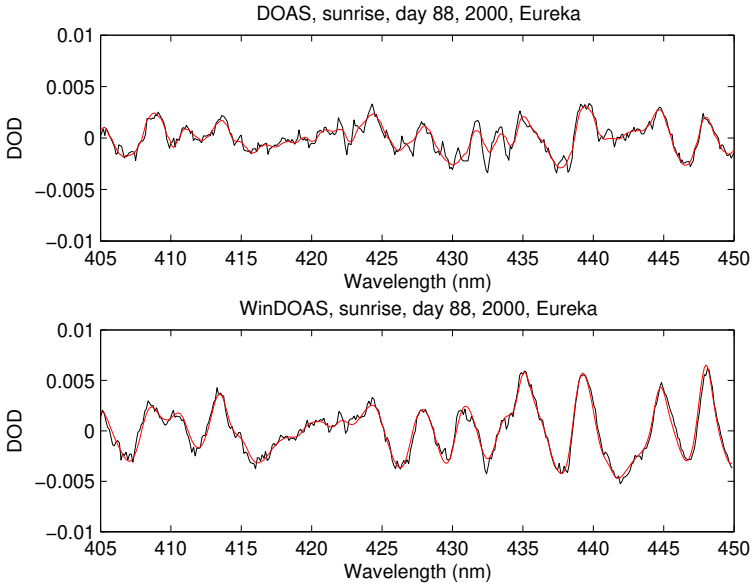

Fig. 3. Differential optical depths for NO_2 (measured in black and fitted in red) at SZA 90° for UT-GBS zenith-sky measurements made on day 88 (28 March 2000), sunrise at Eureka: (top) using the existing DOAS software and (bottom) using WinDOAS software.

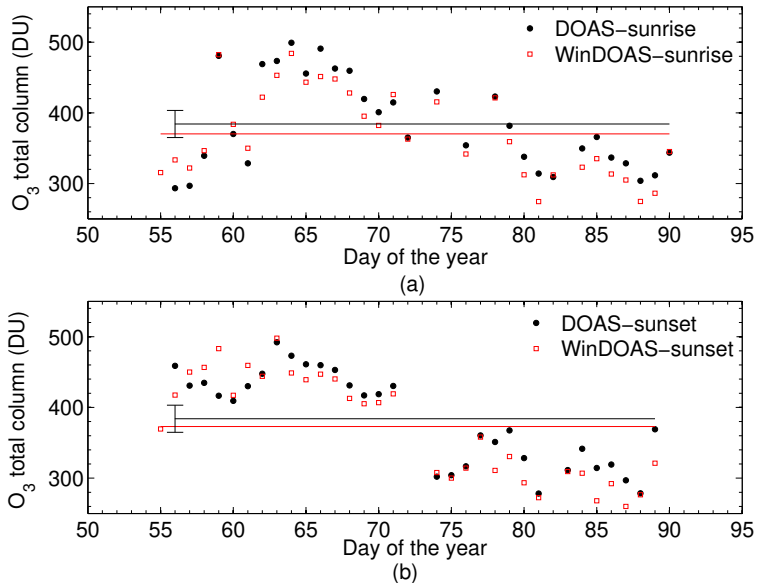

Fig. 4. The retrieved O_3 VCDs for UT-GBS zenith-sky measurements for (top panel) sunrise and (bottom panel) sunset during winter/spring 2000 at Eureka, obtained using DOAS and WinDOAS. The black solid lines show the DOAS mean O_3 VCD and the red lines show the WinDOAS mean O_3 VCD; the error bar indicates ±5%.

AMTD
2, 343–377, 2009

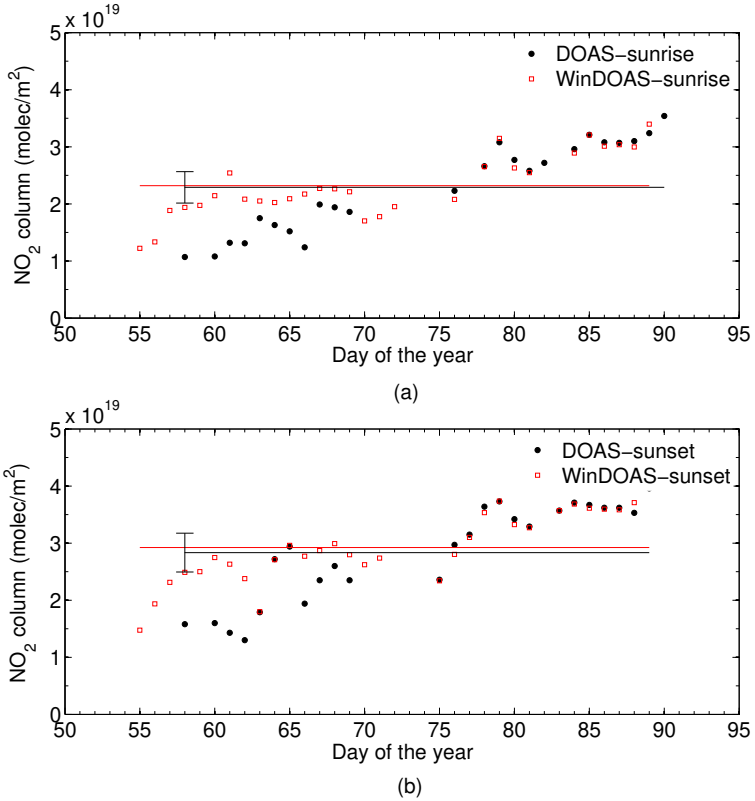

Fig. 5. The retrieved NO_2 VCDs for UT-GBS zenith-sky measurements for (top panel) sunrise and (bottom panel) sunset during winter/spring 2000 at Eureka, obtained using DOAS and WinDOAS. The black solid lines show the mean DOAS NO_2 VCD and the red lines show the WinDOAS mean NO_2 VCD; the error bar indicates ±12%.

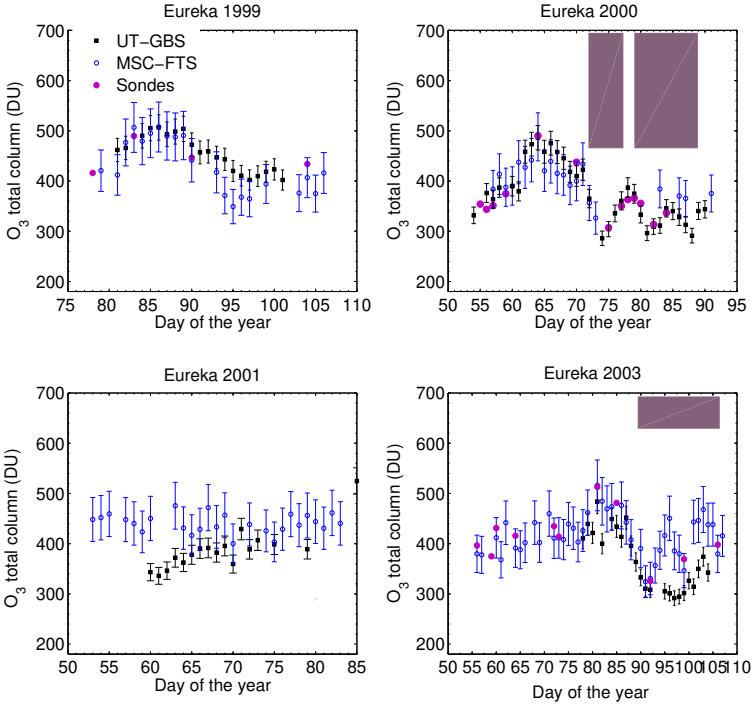

Fig. 6. Daily mean O_3 total columns during winter/spring 1999, 2000, 2001 and 2003. The periods when Eureka was inside the vortex are indicated by the shaded blocks.

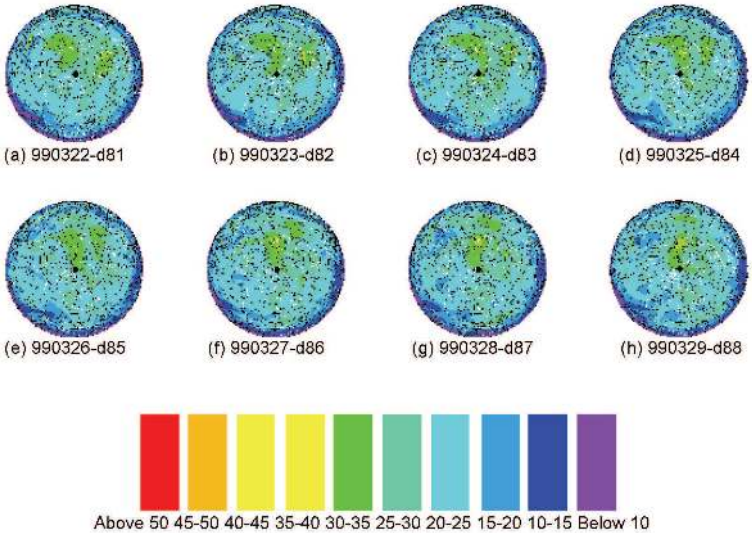

Fig. 7. ECMWF PV ($\times 10^{-5}$ Km^2 kg^{-1} s^{-1}) maps of the Northern Hemisphere at 475 K during March 1999. The location of Eureka is marked with a black dot. The polar vortex during 1999 was weak and not much variation is seen in PV.

AMTD
2, 343–377, 2009

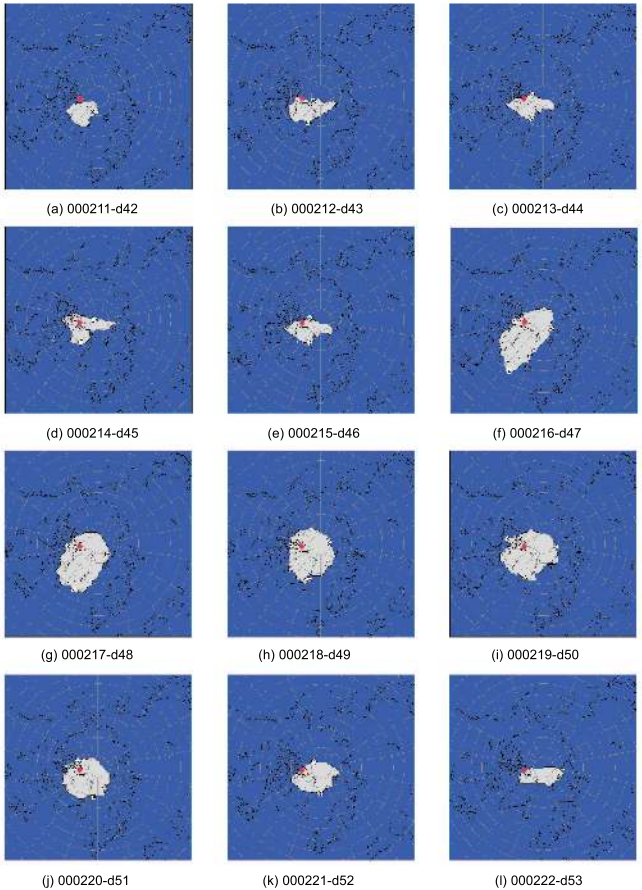

Fig. 8. ECMWF maps of potential PSC areas in the Northern Hemisphere at 475 K during February 2000. The location of Eureka is marked with a red dot.

AMTD
2, 343–377, 2009

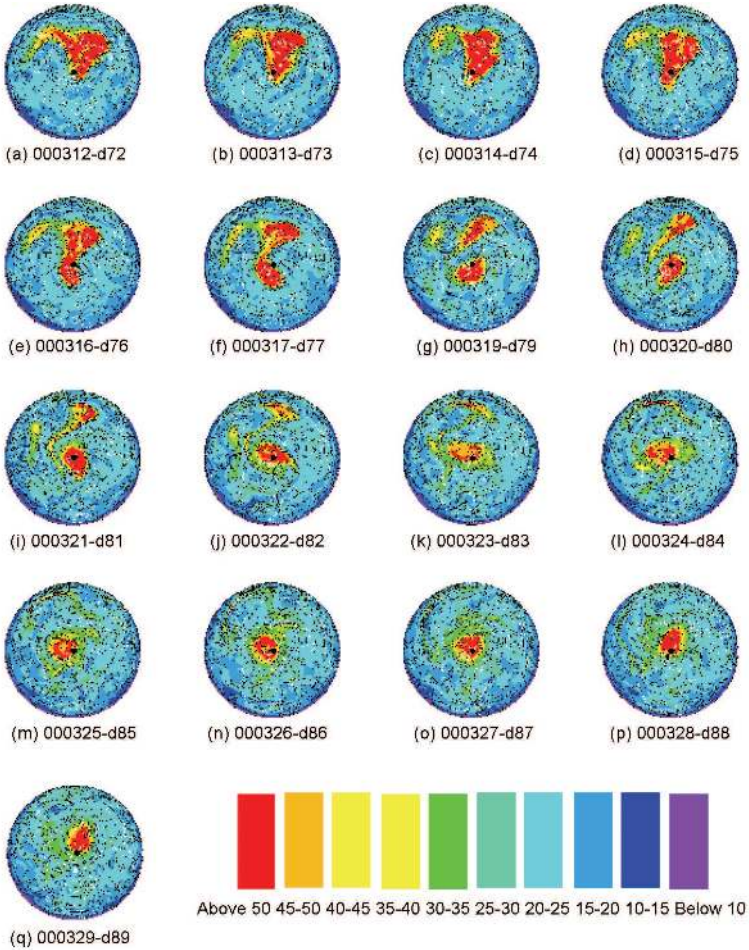

Fig. 9. ECMWF PV ($\times 10^{-5}$ Km^2 kg^{-1} s^{-1}) maps of the Northern Hemisphere at 475 K during March 2000. The location of Eureka is marked with a black dot.

AMTD
2, 343–377, 2009

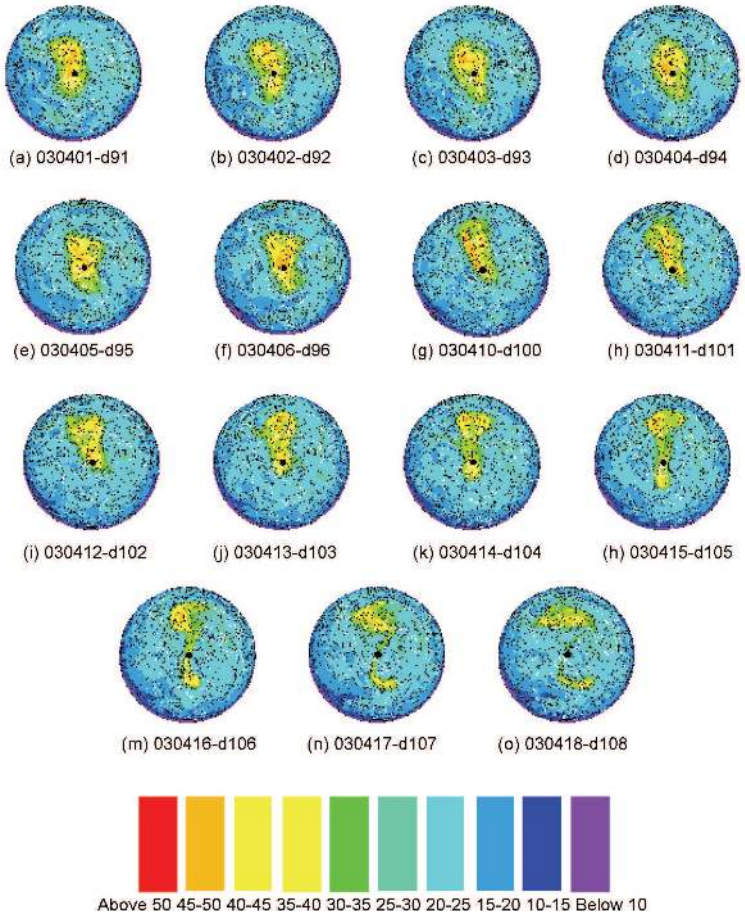

Fig. 10. ECMWF PV maps of the Northern Hemisphere at 475 K during April 2003. The location of Eureka is marked with a black dot.

AMTD
2, 343–377, 2009

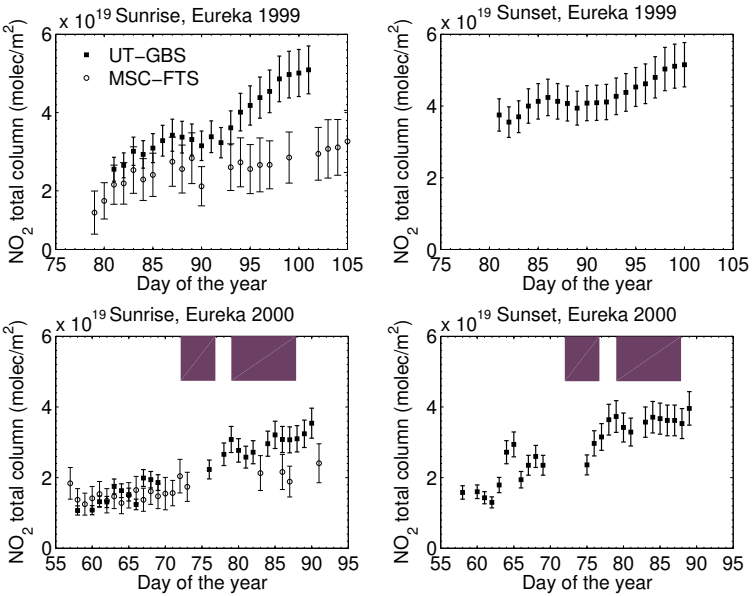

Fig. 11. NO_2 total columns during sunrise and sunset (SZA=90°) for winter/spring 1999 and 2000 at Eureka. MSC FTS measurements are plotted with UT-GBS sunrise measurements as they are closer in time to these measurements. The periods when Eureka was inside the vortex are indicated by the shaded blocks.

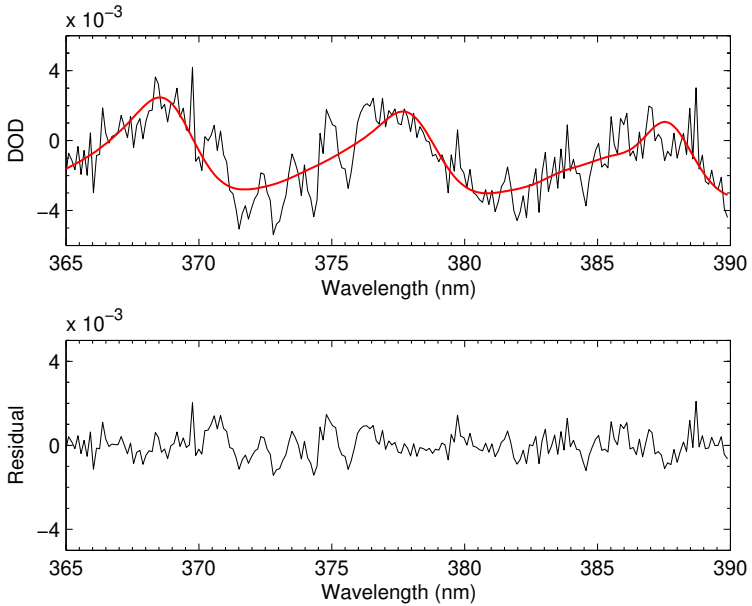

Fig. 12. Differential optical depths (measured in black and fitted in red) and fit residuals (the bottom panel) for OClO at 90° SZA for UT-GBS zenith-sky measurements during 2000 made on day 88 (28 March 2000), sunrise at Eureka.

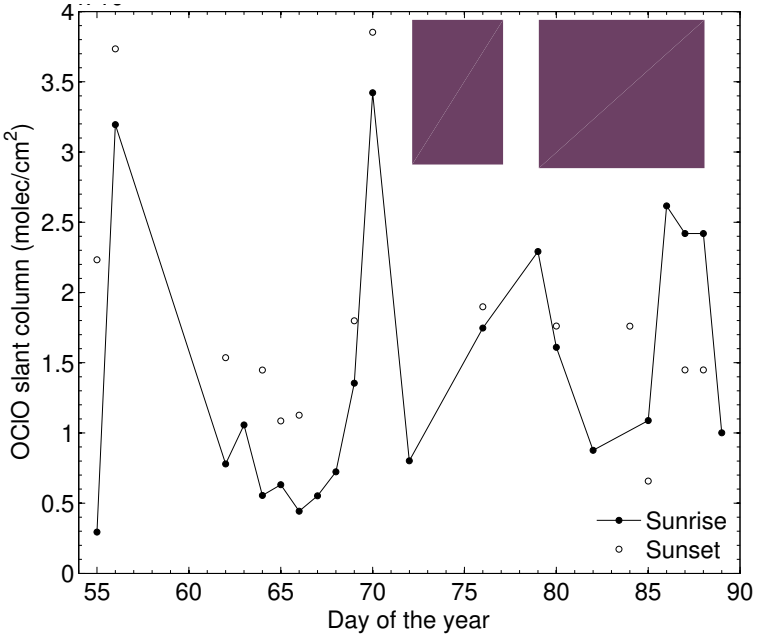

Fig. 13. The OClO DSCDs during winter/spring 2000. The periods when Eureka was inside the vortex are indicated by the shaded blocks.